Zeolite Catalysis

DOI: 10.1002/anie.201109026

X-ray Imaging of Zeolite Particles at the Nanoscale: Influence of Steaming on the State of Aluminum and the Methanol-To-Olefin Reaction**

*Luis R. Aramburo, Emiel de Smit, Bjørnar Arstad, Matti M. van Schooneveld, Linn Sommer, Amélie Juhin, Tadahiro Yokosawa, Henny W. Zandbergen, Unni Olsbye, Frank M. F. de Groot, and Bert M. Weckhuysen**

In view of the limited oil reserves the methanol-to-olefin (MTO) process is an interesting catalytic route to provide raw materials for chemical industries. In the last decades, a vast number of studies have been devoted to increase our understanding of this important catalytic reaction leading to a consensus concerning the mechanism.[1–4] Accordingly, MTO is thought to proceed through the so-called "hydrocarbon pool" (HCP) mechanism,[5,6] in which methanol is added to an organic scaffold present within the zeolite framework. This is followed by elimination of olefinic species in a closed catalytic cycle. Microporous silicoaluminophosphates and aluminosilicates, such as SAPO-34 and ZSM-5, are often used as MTO catalysts because of their unique acidic and structural properties. In the case of ZSM-5 the formation of ethene and propene is governed by two different catalytic routes,[7,8] allowing in principle to control the ethene/propene ratio. Unfortunately, throughout the MTO reaction undesired carbon deposits are formed in the narrow micropore system of ZSM-5, leading to severely restricted diffusion and therefore limited catalytic activity.[9] To overcome these limitations efforts have been made to improve the pore accessibility during synthesis,[10–12] and/or in post-synthetic steps,[13,14] resulting in significant improvements in the diffusion properties of ZSM-5.

In this work, two commercial ZSM-5 zeolites with dimensions of approximately 200–800 nm have been studied by scanning transmission X-ray microscopy (STXM). The first sample, denoted as ZSM-5-C, was calcined for 6 h at 550 °C, whereas the second sample, further labeled as ZSM-5-S, was steamed for 3 h at 700 °C. Details on the preparation and characteristics of ZSM-5-C and ZSM-5-S can be found in the Supporting Information (Figures S1–S13, Tables S1–S6). We will show how STXM, in combination with bulk characterization techniques, allows investigating the physicochemical properties of ZSM-5 zeolites in a novel way at the nanoscale.[15,16] More specifically, detailed chemical maps, with a spatial resolution of 70 nm, have been obtained of aluminum, oxygen, and carbon, even under realistic reaction conditions.[17–19] In this manner, the influence of steaming on the state of aluminum, that is, the coordination and spatial distribution, as well as on the MTO performance, has been unraveled.

In a first set of experiments, STXM was applied to characterize the X-ray absorption of ZSM-5-C and ZSM-5-S at the O, Si, and Al K-edge. The obtained spectra are presented in Figure 1, showing important changes in the Al environment after steaming. The Al K-edge X-ray absorption (XA) spectrum of ZSM-5-C showed a sharp white line located at 1565.5 eV and a broad peak present at 1580 eV related to medium range order.[20] In contrast, the Al K-edge XA spectrum of ZSM-5-S disclosed the appearance of new features at 1567 and 1570 eV characteristic of higher Al coordination states.[21] As the intensity and shape of these features are strongly influenced by the local electronic structure around the absorber,[20–22] the comparison with reference compounds is helpful.[23,24] To this end, the experimental Al K-edge XA spectra of ZSM-5-C and ZSM-5-S were fitted with a linear combination of the XA spectra of three reference compounds, namely albite (four-fold Al mineral), berlinite (four-fold Al mineral), and andalusite (mineral with five- and six-fold Al). The obtained results, along with details concerning the fitting procedure, are presented in the Supporting Information. Overall, the spectral fitting indicated that ZSM-5-C contained mainly four-fold Al, next to minor amounts of five- and six-fold Al. In contrast

[*] L. R. Aramburo, Dr. E. de Smit, M. M. van Schooneveld, Dr. A. Juhin, Prof. Dr. F. M. F. de Groot, Prof. Dr. B. M. Weckhuysen
Inorganic Chemistry and Catalysis Group
Debye Institute for Nanomaterials Science
Utrecht University, Universiteitslaan 99
3584 CG Utrecht (The Netherlands)
E-mail: b.m.weckhuysen@uu.nl

Dr. T. Yokosawa, Prof. Dr. H. W. Zandbergen
Kavli Institute of NanoScience
National Centre for High Resolution Electron Microscopy
Delft University of Technology
PO Box 5046, 2600 GA Delft (The Netherlands)

Dr. L. Sommer, Prof. Dr. U. Olsbye
Centre for Materials Science and Nanotechnology
Department of Chemistry, University of Oslo
0315 Oslo (Norway)

Dr. B. Arstad
Department of Hydrocarbon Process Chemistry
SINTEF Materials & Chemistry, 0314 Oslo (Norway)

[**] We thank the NRSC-C (B.M.W.), the NWO-CW Top (B.M.W.), and the NWO-CW VICI (F.M.F.d.G.) for financial support and D. Cabaret (IMPMC, Université Pierre et Marie Curie) for providing the aluminum references. T. Tyliszczak (Lawrence Berkeley National Laboratory), J. Wang (Canadian Light Source), S. Svelle (University of Oslo), and A. M. J. van der Eerden (Utrecht University) are kindly thanked for their contributions.

Supporting information for this article is available on the WWW under http://dx.doi.org/10.1002/anie.201109026.

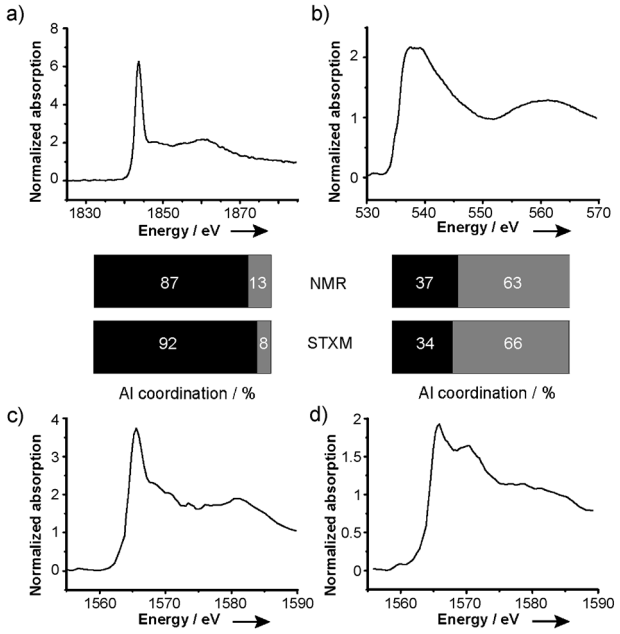

Figure 1. a) Si, b) O, and c) Al K-edge X-ray absorption spectra of ZSM-5-C and d) Al K-edge XA spectrum of ZSM-5-S. The bar graphs represent the percentage estimation of four-fold Al (black) with respect to five- and six-fold Al species (grey) for ZSM-5-C (left) and ZSM-5-S (right), as measured with STXM and NMR spectroscopy.

the relative contributions of each reference compound were significantly altered (Table S6 in the Supporting Information) and a much higher amount of five- and six-fold Al was found in ZSM-5-S. Moreover, the contribution of albite and berlinite changed to a great extent, indicating a variation in the four-fold Al environment. The less well-defined region, located 15–20 eV above the white line in the Al K-edge XA spectrum of ZSM-5-S, supports this conclusion.

To corroborate the STXM results independent ^{27}Al magic angle spinning (MAS) NMR spectroscopy was performed on ZSM-5-C and ZSM-5-S. The results are summarized in Figure S7 in the Supporting Information. The NMR spectrum of ZSM-5-C showed resonances that can be directly attributed to four- and six-fold Al, located in the region of 60–50[25–27] and 0 ppm,[25–27] respectively. In contrast, the NMR spectrum of ZSM-5-S showed an increase in the amount of six-fold Al at the expense of four-fold Al. A resonance in the region of 30–35 ppm, attributed to five-fold Al was found for ZSM-5-S.[28]

In addition to these findings, a specially designed in situ micro-electromechanical system (MEMS) nanoreactor was used to study the dynamic transformations of Al during the zeolite activation at high temperatures. This allows imaging zeolitic systems under their working conditions, showing the susceptibility of Al to change its coordination with variations in the water content and/or temperature conditions.[29–31] The differences in the spectral features appearing in the Al K-edge XA spectra obtained at room temperature and at 450 °C showed that at high temperatures six- and five-fold Al reverted into four-fold Al (Figure S9 in the Supporting Information). Simultaneously, at 450 °C a pre-edge feature was observed, which can arise because of the presence of three-fold Al[31,32] and/or electronic transitions induced by vibrational effects.[33]

Besides the coordination of the Al species, its spatial distribution is a matter of importance. Until now, this issue has not been fully understood, as a result of the compromise between spatial resolution and chemical information often faced by most of the microspectroscopic techniques employed. STXM, however, offers an attractive way to elucidate differences in both the coordination and spatial distribution of Al at the nanometer scale. For this purpose, the obtained Al energy stacks, with a spatial resolution of 70 nm, were fitted with the set of reference compounds used for spectral fitting. The results, depicted in Figure 2, showed a homogeneous 2D distribution of four-fold Al with respect to

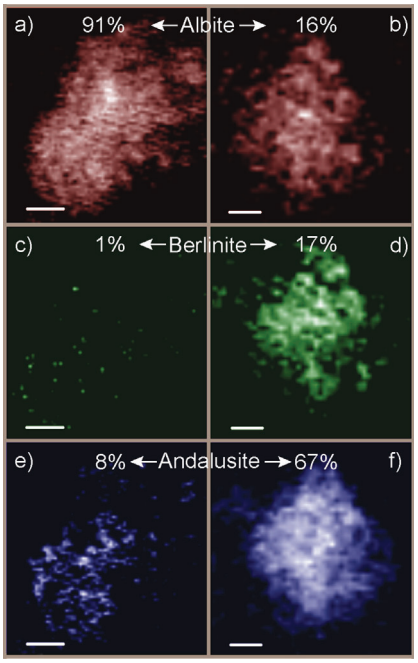

Figure 2. Aluminum coordination and spatial distribution in ZSM-5-C (a, c, and e) and ZSM-5-S (b, d, and f).The different contributions have been obtained by fitting the energy stacks with the Al K-edge XA spectra of albite (a–b, red), berlinite (c–d, green), and andalusite (e–f, blue). The scale bar represents 500 nm in (a, c, and e) and 1 μm in (b, d, and f).

higher Al coordination environments in ZSM-5-C. Analogously, this was the case for ZSM-5-S, though the contribution of higher Al coordination environments was considerably higher than that of four-fold Al. Furthermore, it was found that the contribution of albite and berlinite were equally divided and homogeneously distributed throughout the ZSM-5-S zeolite aggregate (Figure 2 b,d).

With the aim of assessing how the aforementioned variations in the state of aluminum render into the catalytic performance during MTO, both samples were tested under realistic reaction conditions. Further details concerning the catalytic testing can be found in the Supporting Information. The obtained results, displayed in Figure 3, showed an initial

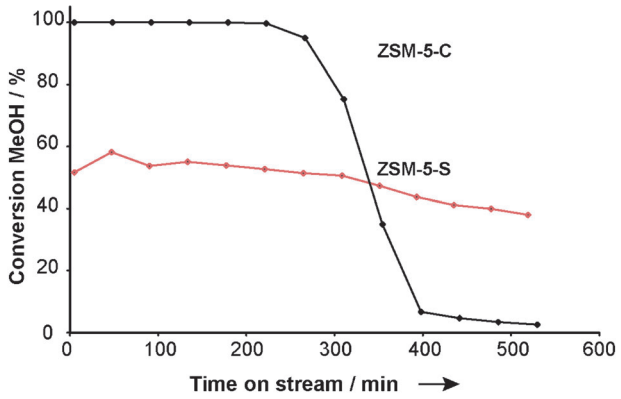

Figure 3. Methanol conversion versus time on stream for ZSM-5-C (black) and ZSM-5-S (red) obtained from the catalytic test performed at 500 °C.

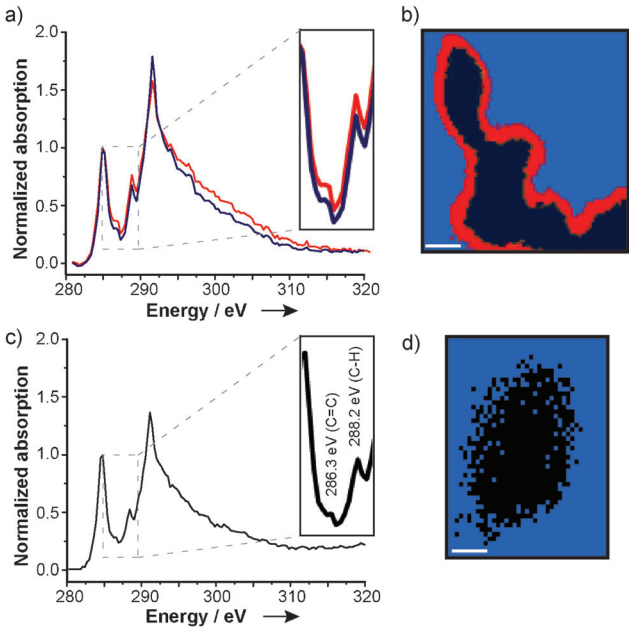

Figure 4. Carbon K-edge XA spectra of a) ZSM-5-C and c) ZSM-5-S, obtained from the cluster analysis performed after 150 min of time on stream. Cluster index for b) ZSM-5-C and for d) ZSM-5-S. The scale bar represents 250 nm in both cases.

methanol conversion close to 100% for ZSM-5-C, being active for more than 230 min. Subsequently, the activity was reduced, leading to a fully deactivated catalyst. Unlike ZSM-5-C, the starting conversion of methanol in ZSM-5-S was close to 60% and the activity was reduced by less than 20% within 500 min of the reaction, disclosing a higher resistance towards deactivation. As interestingly were the differences in selectivity between both samples. Figure S8 in the Supporting Information showed that ZSM-5-C mainly led to the formation of C6+ products, whereas the dominant product for ZSM-5-S was propene. This indicates that ZSM-5-C operates through the aromatic-based HCP mechanism, whereas the alkene-based HCP mechanism is dominating in the ZSM-5-S material.

To gain insight into whether the differences shown in activity and selectivity were related to local heterogeneities in the hydrocarbon formation, STXM was applied to characterize ZSM-5-C and ZSM-5-S under reaction conditions. To this end, the C stacks were measured after 150 min in the reaction stream. Subsequently, a principal component analysis (PCA) was used to create a covariance matrix from the stack data and in a second step a cluster analysis was performed to classify the pixels accordingly to similarities in their spectra. The results of this analysis are presented in Figure 4a, showing the presence of two different C K-edge XA spectra for ZSM-5-C, which originated from distinct regions of the aggregate. Among the features present in the C XA spectra, those appearing at 285, 287.6–288.2, and 291–293.5 eV correspond to transitions from the C 1s to the unoccupied C=C σ*,[34–37] C–H σ*,[36–38] and C–C σ*[39,40] molecular orbitals. Additionally, the peak appearing between 286 and 287 eV is attributed to transitions of a core electron to the unoccupied C=C σ* molecular orbitals, arising because of the presence of non-quivalent C atoms in an sp^2 hybridization state.[41] Importantly, the latter transitions can be used as a fingerprint of the MTO coke precursor species in the C XA spectra as they originate from aromatic species with high symmetry (i.e., naphthalene and anthracene).

Interestingly, as shown in Figure 4b, a relative increase in the transitions appearing between 286 and 287 eV was observed in the outer regions of ZSM-5-C, leading to a core–shell distribution of hydrocarbon species within the zeolite aggregate. More specifically, ZSM-5-C displayed a shrinking C shell in which the bulkier hydrocarbons were preferentially located in the outer rim of the zeolite aggregate. The relative increase observed in the peak located between 287.6 and 288.2 eV with respect to the 285 eV peak supports this observation. To further verify the existence of this carbon shell, the experimental C K-edge XA spectra were compared with a series of reference compounds differing in the number of non-equivalent C atoms. The results are given in Figure S13 in the Supporting Information, confirming the C shell model for ZSM-5-C. In contrast, the cluster analysis performed on ZSM-5-S indicated the presence of a single C XA spectrum, as shown in Figure 4c, which implied a homogeneous spatial distribution of the generated hydrocarbon species within this aggregate. This is further illustrated in Figure 4d.

The higher resistance towards deactivation shown by ZSM-5-S can be rationalized by the property changes induced by steaming. In particular, the lower acid site strength of ZSM-5-S (Figure S4 in the Supporting information) may explain the reduced speed in the formation of coke precursor species.[42,43] Simultaneously, the improved diffusion properties of ZSM-5-S (Figures S2–S3 in the Supporting Information) lead to a more homogeneous formation of hydrocarbon species within this catalyst aggregate, as shown by the superposition of the C and O chemical maps of Figure S10 in the Supporting Information. As a result, the reduced acidity and increased pore accessibility of ZSM-5-S lead to a more stable catalyst material, which contains hydrocarbon species homogeneously distributed within the aggregate.

Summarizing, a powerful nanoscale chemical imaging method has been successfully combined with bulk character-

ization techniques, such as ^{27}Al MAS NMR spectroscopy. In this manner, important insights into the influence of steaming on commercial ZSM-5 zeolites have been obtained. For example, information on the variations in the Al coordination and spatial distribution could be revealed, whereas the use of an in situ reactor demonstrates that five- and six-fold Al revert into lower coordination states at high temperatures. Furthermore, during MTO it was possible to measure C spectra under reaction conditions and on this basis we have been able to construct C maps at the nanoscale. It was found that ZSM-5-S, showing a superior catalytic stability, is represented by a single C spectrum, which can be found in a homogeneous manner within the zeolite aggregate. This is in contrast with the fast deactivation of ZSM-5-C, which can be represented by two C XA spectra inhomogeneously distributed within the zeolite aggregate. More bulky hydrocarbon compounds are present in a shell–core fashion, most probably gradually leading to pore blocking and therefore preventing the material to be accessible for new reactants.

Received: December 21, 2011
Revised: February 9, 2012
Published online: March 1, 2012

Keywords: aluminum · heterogeneous catalysis · olefins · X-ray microscopy · zeolites

[1] W. G. Song, D. M. Marcus, H. Fu, J. O. Ehresmann, J. F. Haw, *J. Am. Chem. Soc.* **2002**, *124*, 3844 – 3845.
[2] D. Lesthaeghe, V. Van Speybroeck, G. B. Marin, M. Waroquier, *Angew. Chem.* **2006**, *118*, 1746 – 1751; *Angew. Chem. Int. Ed.* **2006**, *45*, 1714 – 1719.
[3] D. Lesthaeghe, V. Van Speybroeck, G. B. Marin, M. Waroquier, *Chem. Phys. Lett.* **2006**, *417*, 309 – 315.
[4] D. Lesthaeghe, V. Van Speybroeck, G. B. Marin, M. Waroquier, *Ind. Eng. Chem. Res.* **2007**, *46*, 8832 – 8838.
[5] R. M. Dessau, *J. Catal.* **1986**, *99*, 111 – 116.
[6] I. M. Dahl, S. Kolboe, *J. Catal.* **1994**, *149*, 458 – 464.
[7] M. Bjørgen, S. Svelle, F. Joensen, J. Nerlov, S. Kolboe, F. Bonino, L. Palumbo, S. Bordiga, U. Olsbye, *J. Catal.* **2007**, *249*, 195 – 207.
[8] M. Bjørgen, U. Olsbye, S. Svelle, S. Kolboe, *Catal. Lett.* **2004**, *93*, 37 – 40.
[9] D. M. Bibby, R. F. Howe, G. D. McLellan, *Appl. Catal. A* **1992**, *93*, 1 – 34.
[10] A. Corma, V. Fornes, S. B. Pergher, T. L. M. Maesen, J. G. Buglass, *Nature* **1998**, *396*, 353 – 356.
[11] L. Tosheva, V. P. Valtchev, *Chem. Mater.* **2005**, *17*, 2494 – 2513.
[12] S. Wang, T. Dou, Y. P. Li, Y. Zhang, X. F. Li, Z. C. Yan, *Catal. Commun.* **2005**, *6*, 87 – 91.
[13] J. C. Groen, W. D. Zhu, S. Brouwer, S. J. Huynink, F. Kapteijn, J. A. Moulijn, J. Perez-Ramirez, *J. Am. Chem. Soc.* **2007**, *129*, 355 – 360.
[14] S. van Donk, A. H. Janssen, J. H. Bitter, K. P. de Jong, *Catal. Rev. Sci. Eng.* **2003**, *45*, 297 – 319.
[15] F. M. F. de Groot, E. de Smit, M. M. van Schooneveld, L. R. Aramburo, B. M. Weckhuysen, *ChemPhysChem* **2010**, *11*, 951 – 962.
[16] A. M. Beale, S. D. M. Jacques, B. M. Weckhuysen, *Chem. Soc. Rev.* **2010**, *39*, 4656 – 4672.
[17] E. de Smit, I. Swart, J. F. Creemer, G. H. Hoveling, M. K. Gilles, T. Tyliszczak, P. J. Kooyman, H. W. Zandbergen, C. Morin, B. M. Weckhuysen, F. M. F. de Groot, *Nature* **2008**, *456*, 222 – 239.
[18] E. de Smit, I. Swart, J. F. Creemer, C. Karunakaran, D. Bertwistle, H. W. Zandbergen, F. M. F. de Groot, B. M. Weckhuysen, *Angew. Chem.* **2009**, *121*, 3686 – 3690; *Angew. Chem. Int. Ed.* **2009**, *48*, 3632 – 3636.
[19] J. F. Creemer, S. Helveg, G. H. Hoveling, S. Ullmann, A. M. Molenbroek, P. M. Sarro, H. W. Zandbergen, *Ultramicroscopy* **2008**, *108*, 993 – 998.
[20] P. Ildefonse, D. Cabaret, P. Sainctavit, G. Calas, A. M. Flank, P. Lagarde, *Phys. Chem. Miner.* **1998**, *25*, 112 – 121.
[21] D. Cabaret, P. Sainctavit, P. Ildefonse, G. Calas, A. M. Flank, *Phys. Chem. Miner.* **1996**, *23*, 226 – 226.
[22] Z. Y. Wu, A. Marcelli, A. Mottana, G. Giuli, E. Paris, F. Seifert, *Phys. Rev. B* **1996**, *54*, 2976 – 2979.
[23] G. Calas, G. E. Brown, G. A. Waychunas, J. Petiau, *Phys. Chem. Miner.* **1987**, *15*, 19 – 29.
[24] G. E. Brown, G. Calas, G. A. Waychunas, J. Petiau, *Rev. Mineral.* **1988**, *18*, 431 – 512.
[25] S. M. Campbell, D. M. Bibby, J. M. Coddington, R. F. Howe, R. H. Meinhold, *J. Catal.* **1996**, *161*, 338 – 349.
[26] S. M. Cabral de Menezes, Y. L. Lam, K. Damodaran, M. Pruski, *Microporous Mesoporous Mater.* **2006**, *95*, 286 – 295.
[27] R. Jelinek, B. F. Chmelka, Y. Wu, P. J. Grandinetti, A. Pines, P. J. Barrie, J. Klinowski, *J. Am. Chem. Soc.* **1991**, *113*, 4097 – 4101.
[28] J. Chen, T. Chen, N. Guan, J. Wang, *Catal. Today* **2004**, *93*, 627.
[29] L. A. Bugaev, J. A. van Bokhoven, A. P. Sokolenko, Y. V. Latokha, L. A. Avakyan, *J. Phys. Chem. B* **2005**, *109*, 10771 – 10778.
[30] A. Omegna, R. Prins, J. A. van Bokhoven, *J. Phys. Chem. B* **2005**, *109*, 9280 – 9283.
[31] J. A. van Bokhoven, A. M. J. van der Eerden, D. C. Koningsberger, *J. Phys. Chem. B* **2005**, *109*, 7435 – 7442.
[32] G. Agostini, C. Lamberti, L. Palin, M. Milanesio, N. Danilina, B. Xu, M. Janousch, J. A. van Bokhoven, *J. Am. Chem. Soc.* **2010**, *132*, 667 – 678.
[33] C. Brouder, D. Cabaret, A. Juhin, P. Sainctavit, *Phys. Rev. B* **2010**, *81*, 5619 – 5633.
[34] S. Bernard, O. Beyssac, K. Benzerara, N. Findling, G. Tzvetkov, G. E. Brown, *Carbon* **2010**, *48*, 2506 – 2516.
[35] H. A. Katzman, P. M. Adams, T. D. Le, C. S. Hemminger, *Carbon* **1994**, *32*, 379 – 391.
[36] P. R. Haberstroh, J. A. Brandes, Y. Gelinas, A. F. Dickens, S. Wirick, G. Cody, *Geochim. Cosmochim. Acta* **2006**, *70*, 1483 – 1494.
[37] Y. Zubavichus, A. Shaporenko, V. Korolkov, M. Grunze, M. Zharnikov, *J. Phys. Chem. B* **2008**, *112*, 13711 – 13716.
[38] D. Solomon, J. Lehmann, J. Kinyangi, B. Liang, K. Heymann, L. Dathe, K. Hanley, S. Wirick, C. Jacobsen, *Soil Sci. Soc. Am. J.* **2009**, *73*, 1817 – 1830.
[39] A. P. Hitchcock, D. C. Newbury, I. Ishii, J. Stohr, J. A. Horsley, R. D. Redwing, A. L. Johnson, F. Sette, *J. Chem. Phys.* **1986**, *85*, 4849 – 4862.
[40] A. P. Hitchcock, I. Ishii, *J. Electron Spectrosc. Relat. Phenom.* **1987**, *42*, 11 – 26.
[41] M. L. Gordon, D. Tulumello, G. Cooper, A. P. Hitchcock, P. Glatzel, O. C. Mullins, S. P. Cramer, U. Bergmann, *J. Phys. Chem. A* **2003**, *107*, 8512 – 8520.
[42] S. Svelle, F. Joensen, J. Nerlov, U. Olsbye, K.-P. Lillerud, S. Kolboe, M. Bjorgen, *J. Am. Chem. Soc.* **2006**, *128*, 14770 – 14771.
[43] J. Liu, C. X. Zhang, Z. H. Shen, W. M. Hua, Y. Tang, W. Shen, Y. H. Yue, H. L. Xu, *Catal. Commun.* **2009**, *10*, 1506 – 1509.

